Available online at www.sciencedirect.com

SciVerse ScienceDirect

Proceedings of the Combustion Institute 34 (2013) 1527–1535

Proceedings of the Combustion Institute

www.elsevier.com/locate/proci

Pressure and fuel effects on turbulent consumption speeds of H_2/CO blends

Prabhakar Venkateswaran [a,*], Andrew Marshall [b], Jerry Seitzman [a], Tim Lieuwen [a]

[a] School of Aerospace Engineering, Georgia Institute of Technology, Atlanta 30332-0150, GA, USA
[b] School of Mechanical Engineering, Georgia Institute of Technology, Atlanta 30332-0405, GA, USA

Available online 11 July 2012

Abstract

This paper describes measurements and correlations of turbulent consumption speeds, $S_{T,GC}$, of hydrogen/carbon monoxide (H_2/CO) fuel mixtures over a range of conditions. This work is set within the broader context of understanding the sensitivity of the turbulent flame speed to chemical kinetic and diffusive properties of the reactive mixture. Turbulent consumption speed data were obtained at mean flow velocities, turbulence intensities ($u'_{rms}/S_{L,0}$), equivalence ratios and pressures ranging from 4–50 m/s, 5–45, 0.5–0.8, and 1–10 atm, respectively. Experiments were conducted where the mixture equivalence ratio, ϕ, was adjusted at each fuel composition to have nominally the same calculated un-stretched laminar flame speed, $S_{L,0}$. Consistent with prior studies, these data show both fuel composition and pressure effects on the turbulent flame speed. For example, measured $S_{T,GC}$ values of the 90/10 H_2/CO are about 3 times larger than CH_4 blends having the same $S_{L,0}$, turbulence intensity, and operating conditions. Similarly, the 5 atm data have $S_{T,GC}$ values that are consistently about 1.8 times larger than the 1 atm data, at identical conditions and fuel compositions. These data are correlated with a scaling law derived from quasi-steady leading points concepts using detailed kinetics calculations of highly stretched flames. For a given pressure, these scalings do an excellent job in scaling data obtained across the H_2/CO fuel composition and equivalence ratio range. However, the pressure sensitivities are not captured by this scaling, which may be more fundamentally a reflection of the non-quasi-steady nature of the flame leading points. In support of this argument, we show that the spread in the data can largely be correlated with the ratio of a leading point chemical time scale to a flow time scale.

Keywords: Syngas; Turbulent flame speed; Stretch effects; Leading points; Pressure

1. Introduction

This paper describes recent work to measure and model the turbulent consumption speeds, $S_{T,GC}$, of hydrogen/carbon monoxide (H_2/CO) mixtures. This work is set within the broader context of understanding turbulent flame speed sensitivities to chemical kinetic and diffusive properties

* Corresponding author. Address: Ben T. Zinn Combustion Laboratory, Georgia Institute of Technology, 635 Strong St. NW, Atlanta 30318, GA, USA. Fax: +1 404 463 0888.
E-mail address: pvenkatesw3@gatech.edu (P. Venkateswaran).

1540-7489/$ - see front matter © 2012 The Combustion Institute. Published by Elsevier Inc. All rights reserved.
http://dx.doi.org/10.1016/j.proci.2012.06.077

Nomenclature

D	Burner diameter
δ_F	Flame thickness
κ	Stretch rate
κ_{ext}	Extinction stretch rate
l_M	Markstein length
ϕ	Equivalence ratio
S_L	Stretched laminar flame speed
$S_{L,0}$	un-stretched laminar flame speed
$S_{L,LP}$	Leading point laminar flame speed
$S_{L,max}$	Maximum stretched laminar flame speed
S_T	Turbulent flame speed
$S_{T,GC}$	Global turbulent consumption speed
T	Temperature
T_b	Temperature of burnt gases
T_u	Temperature of unburnt gases
τ_{flow}	Flow time defined as D/U_0
$\tau_{S_{L,0}}$	Chemical time scale defined as $\tau_{S_{L,0}} = \frac{\delta_F\vert_{S_{L,0}}}{S_{L,0}}$
$\tau_{S_{L,max}}$	Chemical time scale defined as $\tau_{S_{L,\max}} = \frac{\delta_F\vert_{S_{L,\max}}}{S_{L,\max}}$
U_0	Mean axial velocity
u'_{rms}	mean square turbulence fluctuations
x	Distance along flame normal
ω	Frequency

of the reactive mixture. For example, the effect of fuel composition on the turbulent flame speed is well-documented in the literature [1,2]. Kido et al. [3,4] obtained data for mixtures of H_2, methane (CH_4), and propane (C_3H_8) where, by adjusting the dilution and stoichiometries of the different fuel blends, they obtained different mixtures with the same un-stretched laminar flame speed, $S_{L,0}$. Their data clearly show that these mixtures have substantially different turbulent flame speeds, with the high H_2 mixture having *an order of magnitude* larger S_T value than the propane mixture at the same turbulence intensity. Similarly, other data sets also exist showing strong sensitivities of S_T to fuel composition [1,5–7]. In the same way, other data sets show sensitivities of S_T to pressure and fuel/air ratio that cannot be correlated with the corresponding laminar, un-stretched flame speeds of the mixtures [8,9].

Prior studies have shown that the sensitivity of the turbulent flame speed to fuel composition is associated with the stretch sensitivity of the reactant mixture, which leads to variations in the local consumption speed along the flame front. In particular, the high mass diffusivity of H_2 makes syngas mixtures highly stretch sensitive. Stretch effects can be manifested through both non-unity Lewis number and preferential diffusion effects [10]. While various modeling approaches have been put forth to capture these effects, conceptual models based on leading points concepts appear to be one of the most natural approaches for capturing these stretch sensitivities [1,11–13]. Leading points are loosely defined as positively curved points on the flame front that propagate out farthest into the reactant mixture. It has been hypothesized that the velocity of these points controls the overall propagation velocity of the turbulent flame [1]; i.e., the turbulent flame speed can be written as:

$$S_T = \langle S_L \rangle_{LP} + \langle u'_{rms} \rangle_{LP} \tag{1}$$

where $\langle\rangle_{LP}$ denotes the ensemble averaged value of the quantity at the flame leading edge. This simplified expression should obviously be interpreted for scaling of local turbulent displacement speeds only [14], and not as a quantitative expression for turbulent flames in general. Thus, the ensemble averaged laminar burning velocity of the turbulent flame leading point, $\langle S_L \rangle_{LP}$, turns out to be a very significant way in which diffusive and kinetic mixture properties influence the turbulent flame speed, and is the focus of the rest of this introduction.

For negative Markstein length, l_M, mixtures, the burning velocity of this positively curved leading point is greater than the laminar un-stretched value [10]. Thus, we can write the inequality:

$$S_{L,0} < \langle S_L \rangle_{LP} < S_{L,\max} \tag{2}$$

where $S_{L,max}$ is the maximum possible burning velocity of a stretched flamelet. For example, $S_{L,max}$ is indicated in Fig. 3 for a positively stretched, steady-state, H_2/CO stagnation flame. Using this inequality, we can write Eq. (1) as:

$$\frac{S_T}{S_{L,\max}} \leq 1 + \frac{\langle u'_{rms} \rangle_{LP}}{S_{L,\max}} \tag{3}$$

The resulting expression is very similar to the classical Damköhler turbulent flame speed scaling [15], except the parameter arising from the analysis is $S_{L,max}$ [14]. Lipatnikov and Chomiak [16] argued that the flame leading points were "critically stretched flamelets", which basically suggests that $\langle S_L \rangle_{LP}$ should be scaled with the respective values of the mixture at very high stretch rates; i.e., that $\langle S_L \rangle_{LP} = S_{L,\max}$ .This expression can be derived rigorously for an isothermal, negative Markstein length flame propagating into a quiescent mixture, where it can be shown that the leading edge of the flame accelerates until settling at

the steady-state value where $S_{L,LP} = S_{L,\max}$ [14].This result follows from the fact that $S_{L,0}$ is a 'repelling' point for thermodiffusively unstable (i.e., $l_M < 0$) flames, since a positively curved perturbation on a flat flame grows with increasing curvature and correspondingly increasing flame speeds. Moreover, $S_{L,max}$ is a stable 'attracting' point for constant density flames with positively curved wrinkles. Thus, in this limit, we can replace the inequality in Eq. (3) with:

$$\frac{S_T}{S_{L,\max}} = 1 + \frac{\langle u'_{rms} \rangle_{LP}}{S_{L,\max}} \tag{4}$$

Note the important caveats in the prior paragraph associated with the applicability of this expression; namely, that the flame leading point be quasi-steady, that gas expansion effects are negligible, and that the mixture has a negative Markstein length. For example, quasi-steadiness of the leading point implies that turbulent eddies must evolve over a time scale that is slow relative to that required for the leading points to be attracted to the $S_{L,max}$ point and for the internal chemical kinetic processes to equilibrate to the evolving flame stretch rate characteristics. In flames with fluctuating stretch rates the augmentation of the laminar burning velocity by positive stretch decreases and the extinction stretch rate increases [17]. Thus, there are two important non-quasi-steady effects which influence this scaling; one related to the geometry of the turbulent flame brush and the other related to the internal flame structure.

In a prior paper, we showed excellent collapse of a range of H_2/CO data using $S_{L,max}$ values obtained from steady-state, detailed kinetics calculations of a premixed, opposed-flow flame [14]. This paper further analyzes the scaling relation given by Eq. (3) as well as coupled pressure and fuel effects. Measuring pressure sensitivities of the turbulent flame speed is a convenient way to probe internal flame structure unsteady effects, as characteristic chemical kinetic times, τ_{chem}, are generally inversely proportional to pressure. There are limited data of this kind in the literature and the results are not well understood. Kobayashi et al. [18] reported turbulent consumption speed measurements of $\phi = 0.9$ CH_4/air mixtures and showed that $S_{T,GC}/S_{L,0}$ increased with pressure due to decreases in$S_{L,0}$, but that $S_{T,GC}$ itself was independent of pressure. Kitagawa et al. [9] reported similar measurements on turbulent flame speeds of H_2/air mixtures at pressures from 1–5 atm; i.e., that $S_T/S_{L,0}$ was primarily sensitive to pressure through influences on $S_{L,0}$. However, the influence on S_T is unclear. Daniele et al. [8] reported $S_{T,GC}$ measurements of H_2/CO mixtures for pressures of 1–20 atm at 623 K. They found that $S_{T,GC}/S_{L,0}$ increased with pressure at each given H_2/CO ratio and $u'_{rms}/S_{L,0}$ value.

In this paper, we report $S_{T,GC}$ measurements at 5 and 10 atm and compare them to previously obtained 1 atm measurements [14]. We show that data can be collapsed quite well using Eq. (4) for a given pressure, but that significant differences are observed across different pressures. Previously, Kobayashi et al. [18] suggested that the rise in $S_{T,GC}/S_{L,0}$ with pressure at low $u'_{rms}/S_{L,0}$ in their data was due to the amplification of the Darrieus-Landau (D-L) instability. They also suggest that the thinning of the flame and decreasing turbulent Gibson scale with pressure allows the flame to interact with a large range of turbulent length scales, resulting in finer scale wrinkling and, hence, larger flame area. However, the D-L instability probably does not have a dominant influence on the burning velocity at high turbulence intensities [18], where we also show that the pressure effect persists. Pressure also has strong impacts on mixture stretch sensitivities, such as Markstein length, l_M. However, the data presented in this paper clearly shows that the mixture stretch sensitivity, as parameterized by the steady-state value of l_M or $S_{L,max}$, does not capture the pressure sensitivity of the S_T. We suggest that this scatter reflects non-quasi-steady effects and show that much of the scatter can be collapsed by a two-factor parameterization of S_T based on the mixture stretch sensitivity and chemical time. In other words, we suggest that pressure effects on the turbulent burning velocity are more a manifestation of its influence on relative values of turbulence and flame time scales than length scales.

2. Experimental facility and flow field characterization

The turbulent flame speed is a definition dependent quantity and this study focuses on measurements of the turbulent consumption speed, $S_{T,GC}$, using a turbulent Bunsen flame, which is a measurement approach recommended by Gouldin and Cheng [19].

The experimental facility and processing methodologies have been detailed in our previous work [14,20], so only a short description is provided here. A schematic of the system is shown in Fig. 1. The burner is a smoothly contoured nozzle with high contraction ratio to inhibit boundary layer growth and achieve a top-hat exit velocity profile. Measurements were taken with a 12 mm diameter burner. An annular sintered plate around the burner outlet holds a premixed, methane-air pilot flame to stabilize the main flame. The total mass flowrate of the pilot does not exceed 5% of the main flowrate to ensure minimal impact of the pilot on the main flame.

The burner is placed inside a pressure vessel with four orthogonal quartz windows providing viewing areas of 7" × 2". The pilot is lit with a

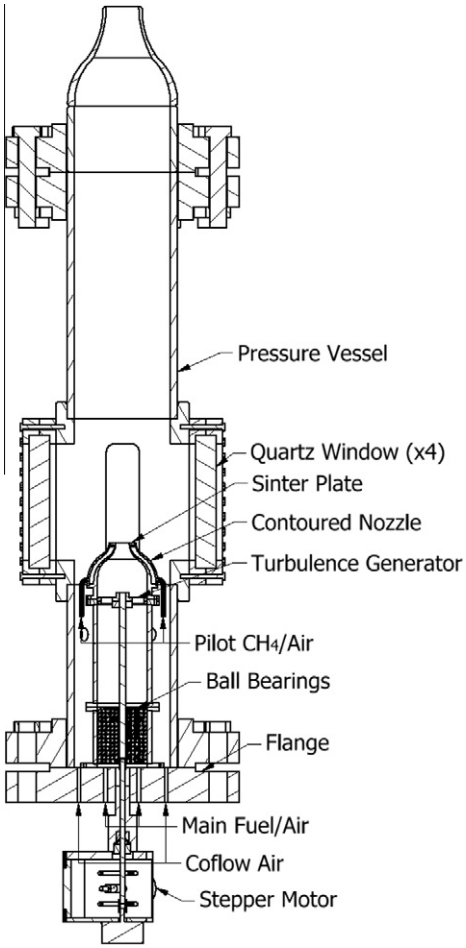

Fig. 1. Schematic of the experimental facility.

hydrogen torch that is ignited using a high voltage spark. The turbulence intensity is varied independently of the mean flow velocity using a remotely operable turbulence generator. Further description of the turbulence generator can be found in Marshall et al. [20].

The flow field was characterized for a wide range of pressure and preheat conditions using 3-component laser Doppler velocimetry (LDV). Only the main conclusions are included here, as complete details may be found in [21].The data show a well-defined top-hat axial velocity profile and low radial and azimuthal velocities. The total centerline turbulence intensity, u'_{rms}/U_0, where u'_{rms} is based upon all three measured velocity components, increased monotonically with blockage ratio (defined as the amount of area blocked by the turbulence generator over the total area). Turbulence intensities were obtained in the range of $u'_{rms}/U_0 = 11$–19%.

3. Experimental conditions and kinetic calculations

3.1. Experimental conditions

Measurements of $S_{T,GC}$ were obtained at 1, 5, and 10 atm as a function of $u'_{rms}/S_{L,0}$ using the 12 mm diameter burner. Data were acquired at mean flow velocities from 20–50 m/s and volumetric H_2/CO ratios from 30/70–90/10, keeping $S_{L,0}$ and reactant temperature fixed at 34 cm/s and 300 K, respectively. $S_{L,0}$ was kept nominally constant for one data set by adjusting the stoichiometry at each H_2/CO ratio and pressure. $S_{L,0}$ estimates were determined using the PREMIX module [22] in CHEMKIN with the Davis H_2/CO mechanism for H_2/CO mixtures [23]. The parameter ranges explored in this study along with the symbol type and color scheme are summarized in Table 1. Figure 2 summarizes where the measured data are located on a Borghi-Peters diagram [24].

3.2. Stretch sensitivity calculations

Stretch sensitivity calculations were performed for the mixtures in Table 1. Stretch sensitivities were calculated using an opposed-flow calculation of two premixed flames with a nozzle separation

Table 1
Investigated parameter space. Pressure data are represented by filled symbols, and the fill color is indicated by the cell color for ϕ in the leftmost column.

	Constant $S_{L,0}$				ϕ Sweep						CH_4
U_0 (m/s)	4, 10, 20, 30, 50										4, 10, 30
H_2 (%)	30	50	70	90	30			60			0
Symbol	○	◁	▷	◇	☆	▽	✡	△	✱	□	✤
ϕ, 1atm	0.61	0.55	0.51	0.48	0.61	0.7	0.8	0.4	0.6	0.8	0.9
ϕ, 5atm	0.75	0.68	0.63	0.59							
ϕ, 10atm		0.75									
$S_{L,0}$ (m/s)	0.34				0.34	0.48	0.59	0.15	0.51	0.9	0.34

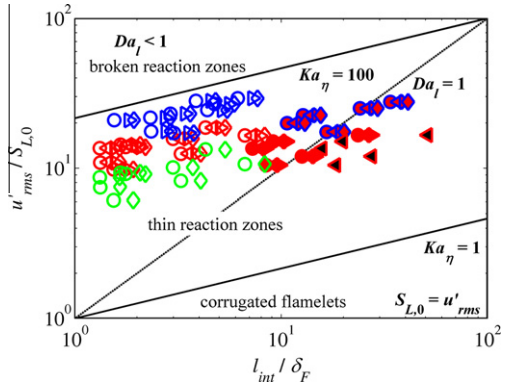

Fig. 2. Borghi-Peters diagram showing location of constant $S_{L,0}$ study data points for the 12 mm burner at 1, 5 and 10 atm.

distance of 20 mm using the OPPDIF [25] module in CHEMKIN. An arc length continuation method was used to determine the extinction point. From these calculations, various stretched properties of the mixture were extracted. In this paper the displacement laminar flame speed is considered, determined from the minimum velocity upstream of the reaction zone, as suggested by Wu and Law [26]. These calculations are performed using detailed kinetics and transport properties which naturally incorporate both non-unity Lewis number and differential diffusion effects.

Figure 3 plots a typical calculation showing the stretch sensitivity of a 30/70 H_2/CO mixture whose $S_{L,0}$ is kept constant at 34 cm/s across the pressures by adjusting the equivalence ratio. At least three global parameterizations of the mixtures stretch sensitivity can be deduced from Fig. 3 - the Markstein length, l_M, the extinction stretch rate, κ_{ext}, and the maximum stretched laminar flame speed, S_{Lmax}. Note the different pressure sensitivities of these three quantities. For example, if pressure is increased by a factor of 5, the extinction stretch rate and Markstein length increase and decrease by a factor of approximately 5, respectively. This can be explained by the thinning of the flame with pressure. In fact, these two effects appear to nearly compensate each other with the result that $S_{L,max}$ is relatively insensitive to pressure. In fact, $S_{L,max}$ remains almost constant above 5 atm and actually decreases beyond 12.5 atm. Although not shown, l_M, S_{Lmax}, and κ_{ext} all increase with H_2 content of the fuel at a given pressure for the constant $S_{L,0}$ sweeps.

4. Results and analysis

4.1. H_2/CO sweeps at constant $S_{L,0}$

This section presents new $S_{T,GC}$ data acquired at 5 and 10 atm, supplementing the 1 atm data previously presented in Ref. [14]. The 1 atm data will be shown alongside this new data in Sec. 4.2. As described earlier, all data were acquired for mixtures where the H_2/CO ratio and equivalence ratio were simultaneously adjusted to maintain the same $S_{L,0}$ value of 34 cm/s. Figure 4 plots $S_{T,GC}$ as a function of u'_{rms} normalized by $S_{L,0}$ for the range of conditions reported in Table 1.Several important observations can be made from this figure. First, fuel effects are clearly present at the elevated pressure conditions, i.e., different H_2/CO blends at constant $S_{L,0}$ and u'_{rms} have different turbulent consumption speeds. For example, at 5 atm and $u'_{rms}/S_{L,0} = 28$, $S_{T,GC}/S_{L,0}$ increases by about 50% as the H_2 content increases from 30% to 90%. A second important observation is the pressure effects. Specifically, $S_{T,GC}$ at 5 atm is approximately double its value at 1 atm, and increases slightly further at 10 atm. This increase is quantified in Fig. 5, which plots the ratio of $S_{T,GC}/S_{L,0}$ at 5 and 10 atm to 1 atm for each mixture and mean flow velocity as a function of turbulence intensity. The figure shows that this ratio has values of about 1.8 and 2.2 at 5 and 10 atm, respectively. Note that this is not an $S_{L,0}$ effect, as $S_{L,0}$ is fixed at 34 cm/s. Furthermore, note that the corresponding low stretch sensitivity of these mixtures, as quantified by l_M actually decreases with pressure, while the high stretch sensitivity, as quantified by $S_{L,max}$ stays relatively constant with pressure. These points will be considered more fully in the next section.

4.2. Analysis: $S_{L,max}$ scaling of data

In this section, the data in Fig. 4 and previously reported 1 atm data are correlated using the quasi-steady scaling law, Eq. (4). Similar calculations as shown in Fig. 3 were performed to normalize the measured turbulent flame speed data, as shown in Fig. 6. This figure shows that both the 1 and 5 atm datasets collapse quite well

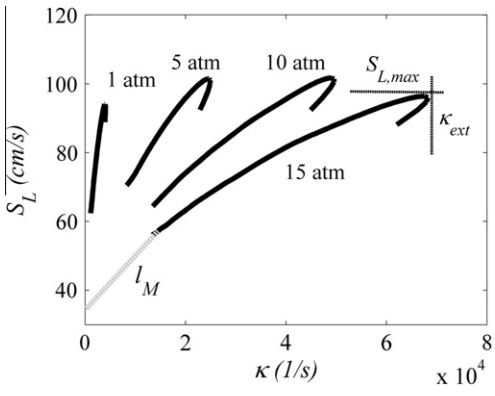

Fig. 3. Pressure effect on mixture stretch sensitivity for 30% H_2 mixtures at constant $S_{L,0}$.

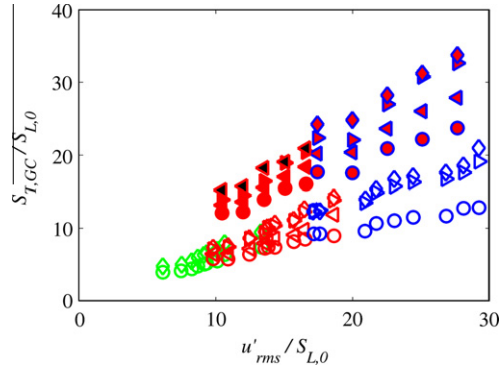

Fig. 4. $S_{T,GC}$ as a function of u'_{rms} normalized by $S_{L,0}$ at various mean flow velocities, H_2/CO ratios, and pressures for the 12 mm diameter burner (See Table 1 for the legend).

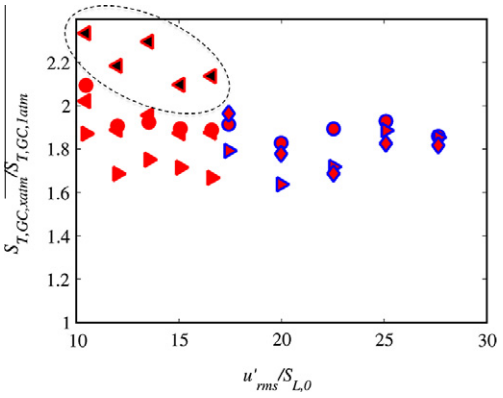

Fig. 5. Ratio of $S_{T,GC}$ at 5 and 10 atm to 1 atm across the range of turbulence intensities investigated. The 10 atm ratio is circled, while the rest are 5 atm ratios.

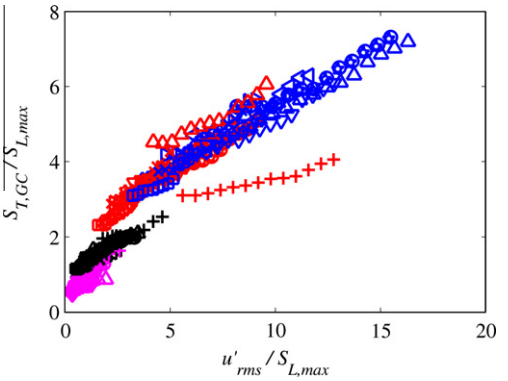

Fig. 7. $S_{T,GC}$ as a function of u'_{rms} normalized by $S_{L,\max}$ for the entire 20 mm burner diameter dataset (See Table 1 for the legend).

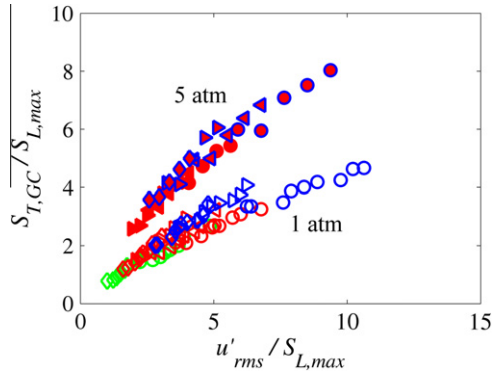

Fig. 6. $S_{T,GC}$ as a function of u'_{rms} normalized by $S_{L,\max}$ at various mean flow velocities, H_2/CO ratios and pressures using the 12 mm diameter burner (See Table 1 for the legend).

individually, but that there are systematic differences between them. Similarly, Fig. 7 plots the normalized 1 atm, 20 mm burner dataset [14]. This normalization produced the interesting result that the 30 m/s CH_4 data did not collapse with the H_2/CO data. However, all constant $S_{L,0}$ data and equivalence ratio sweep data collapse very well.

To summarize, the data taken consistently show that Eq. (4) collapses data across all H_2/CO and equivalence ratio values at a given pressure. However, it does not collapse the 30 m/s CH_4 data, nor does it collapse data taken at different pressures. The next section analyzes potential reasons for this scatter, and particularly focuses on non-quasi-steady chemistry effects.

4.3. Analysis: chemical time scaling of data

In interpreting the factors leading to both the collapse of some data and scatter in others when scaled using Eq. (4), it is important to recall the limitations of this expression summarized in Sec. 1. We believe that the scatter shown in these data stems from the fact that $S_{L,max}$ is not a fundamental property of the mixture. For example, the burning velocity of highly stretched flames is a function of the manner in which the flame is stretched, i.e., by tangential flow straining or curvature [27], as well as the stretch profile through the flame (manifested by, for example, variation in quantities such as $S_{L,max}$ or κ_{ext} with opposed-flow nozzle separation distance or velocity profile [28]). Note that our calculations derive $S_{L,max}$ from a tangentially strained flame, while the actual flame leading points are both curved and strained. We are currently analyzing this further with curved flame computations. In addition, very different $S_{L,max}$ values are obtained when using consumption and displacement based burning velocities [29]. Finally, $S_{L,max}$ is a frequency dependent quantity [17]; the steady-state values used here are only appropriate if the internal structure of the leading point is quasi-steady. We have analyzed several of these points, but do not reproduce the different analyses for sake of space. Instead, we focus on the non-quasi-steady chemistry point, as analysis indicates that of the effects highlighted above, it is chemical time scales that change most significantly with pressure.

In unsteady opposed-flow calculations, Im and Chen [17] show that the absolute value of the Markstein length and $S_{L,max}$ both decrease as the frequency of the imposed strain rate is increased. This dependency can be incorporated into Eq. (1) by replacing $S_{L,max}$ with $S_{L,\max}(\omega)$, which is the frequency dependent $S_{L,max}$. The resulting expression can then be divided by the steady-state $S_{L,max}$ to give:

$$\frac{S_T}{S_{L,\max}} = \frac{S_{L,\max}(\omega)}{S_{L,\max}} + \frac{\langle u'_{rms}\rangle_{LP}}{S_{L,\max}} \tag{5}$$

The degree of non-quasi-steadiness can be determined using the time scale ratio, $\tau_{S_{L,max}}/\tau_{flow}$, where $\tau_{S_{L,max}}$ is a chemical time scale associated with the highly stretched flamelets and τ_{flow} is a characteristic fluid mechanic time scale; i.e., $S_{L,max}(\omega)/S_{L,max} \rightarrow 1$ as $\tau_{S_{L,max}}/\tau_{flow} \rightarrow 0$. The chemical time scale, $\tau_{S_{L,max}}$, is given by $\tau_{S_{L,max}} = \delta_F|_{S_{L,max}}/S_{L,max}$ where $\delta_F|_{S_{L,max}}$ is the flame thickness at SL,max calculated using $\delta_F = (T_b - T_u)/(dT/dx)_{max}$.

The variation in the chemical time scale across H2/CO mixtures and pressures is shown in Fig. 8. The point corresponding to 0% H2 is the pure CH4/air case that was used in the constant SL,0 studies with the 20 mm burner. These data show that pressure exerts the strongest influence on the chemical time. For example, at a fixed H2 content of 30%, there is a factor of about 12 reduction in $\tau_{S_{L,max}}$ associated with a corresponding pressure increase from 1 to 10 atm. In contrast, $\tau_{S_{L,max}}$ increases by about a factor of 3.5 as the H_2 content is increased from 30% to 90% at 1 atm.

Figure 9 plots $S_{T,GC}/S_{L,max}$ as a function of $\tau_{S_{L,max}}/\tau_{flow}$, where $\tau_{flow} = D/U_0$, at fixed turbulence intensities, $u'_{rms}/S_{L,\max} = 3$ and 6.5 for the 12 mm burner data. For reference, the straight lines indicate a power law fit to the data given by $S_{T,GC}/S_{L,max} \sim (\tau_{S_{L,max}}/\tau_{flow})^b$ where $b \sim -0.33$.

Note the clear correlation between turbulent flame speed and time scale ratio across the entire range of pressure and fuel composition. Slower chemistry is associated with lower values of the normalized turbulent flame speed, possibly since the effective $S_{L,max}$ value of the non-quasi-steady flame is lower than its quasi-steady value, as expected from Eq. (5). While the time scale ratios are much less than unity (indicating that the chemistry is actually quasi-steady with respect to the large scales), the corresponding ratios calculated using Kolmogorov time scales range from 20–95 for the same data. In other words, significant non-quasi-steady chemistry effects would be expected for small flow length scale-flame interactions.

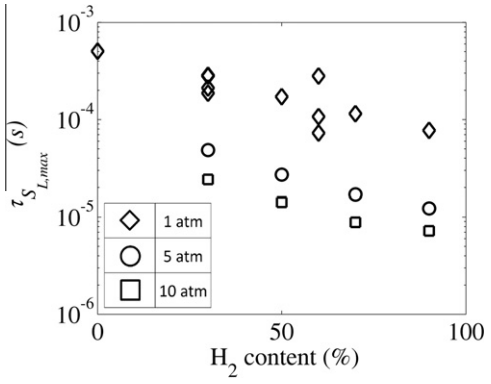

Fig. 8. Variation in $\tau_{S_{L,max}}$ as a function of H_2 content for the different mixtures and conditions investigated. 0% H_2 corresponds to the pure CH_4 mixture.

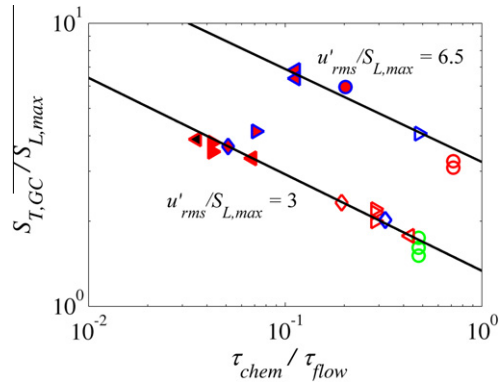

Fig. 9. Dependence of $S_{T,GC}/S_{L,max}$ upon $\tau_{S_{L,max}}/\tau_{flow}$ at a fixed turbulence intensity, $u'_{rms}/S_{L,max} = 3$ and 6.5 for the 12 mm diameter burner.

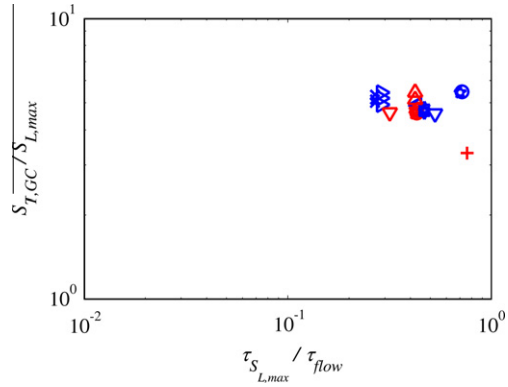

Fig. 10. $S_{T,GC}/S_{L,max}$ as function of $\tau_{S_{L,max}}/\tau_{flow}$ at $u'_{rms}/S_{L,max} = 8$ for the 20 mm diameter burner.

A similar analysis was conducted for the 1 atm data from the 20 mm burner, illustrated in Fig. 7, which showed good correlations except for the 30 m/s CH_4 data. These data and the corresponding H_2/CO blends at the same turbulence intensities are plotted in Fig. 10. Because these data are only taken at one pressure, the range of time scale ratios is much smaller than shown in Fig. 9 and there is almost no variation of normalized turbulent flame speed with fuel composition. Only the much slower CH_4 result stands out. However, its chemical time is quite comparable to the H_2/CO datasets, whose turbulent flame speed values are higher. Further experiments over a broader range of chemical time scales are needed to further understand whether this is an experimental anomaly or an additional effect not accounted for in this scaling.

5. Conclusions

In this paper, we reported turbulent consumption speed measurements of H_2/CO blends at 5 and 10 atm. Experiments were conducted for mean flow velocities of 30 and 50 m/s for H_2/CO blends ranging from 30/70 to 90/10 by volume. It was found that at the same $S_{L,0}$ when the pressure was increased by a factor of 5, the consumption speed increased by almost a factor of 2.

The data were then normalized with $S_{L,max}$ as per the scaling law derived in our earlier work. These data show that, at a given pressure, different fuel compositions and equivalence ratio data collapse. However, systematically different trends are observed with the 5 and 10 atm data. There is some evidence that these systematic differences are more fundamentally due to non-quasi-steady effects, as the pressure differences can be reasonably correlated with a computed chemical time scale for the 12 mm burner. However, the 20 mm, 1 atm data results are less clear because of the smaller range of pressures. Future work will aim to broaden the pressure data to further analyze these sensitivities. In particular, if these pressure effects are fundamentally due to non-quasi-steady effects, then the faster chemistry associated with higher pressure flames suggests that the turbulent flame speed should cease to exhibit a pressure sensitivity at pressures where the flame is internally quasi-steady. Future work is also needed to assess flame brush thickness and progress variable reference surface effects. Specifically, the progress variables used here were extracted from flame chemiluminescence which, for stretch sensitive mixtures, may be expected to be systematically different than progress variables extracted from flame position (such as determined using laser sheet imaging approaches) or average temperature. Moreover, $S_{T,GC}$ is a function of the reference progress variable and, thus, flame brush thickness, which is also influenced by pressure, fuel composition, and measurement quantification approach. Additional work is needed to compare these results using different reference progress variables.

Acknowledgement

This research was partially supported by the University Turbine Systems Research program, Mark Freeman, contract monitor, under contract DE-FC21-92MC29061, by Siemens Energy through a subcontract with DOE prime contract DE-FC26-05NT42644, Dr. Scott Martin contract monitor, and by University of California, Irvine through a subcontract with the California Energy Commission. The authors are grateful to Mr. Bobby Noble, Brad Ochs and Dave Shaw for their invaluable assistance in designing and installing the high pressure test facility. The authors also gratefully acknowledge Mr. Andrew Irby, Daniel Miller, Juan Camilo Pedroza, and Ramon Romero for their assistance in assembling the experimental facility and data collection.

References

[1] A. Lipatnikov, J. Chomiak, *Prog. Energy Combust. Sci.* 31 (1) (2005) 1–73.
[2] J.F. Driscoll, *Prog. Energy Combust. Sci.* 34 (1) (2008) 91–134.
[3] M. Nakahara, H. Kido, *AIAA Journal* 46 (7) (2008) 1569–1575.
[4] H. Kido, M. Nakahara, K. Nakashima, J. Hashimoto, *Proc. Combust. Inst.* 29 (2) (2002) 1855–1861.
[5] D. Littlejohn, R.K. Cheng, *Proc. Combust. Inst.* 31 (2) (2007) 3155–3162.
[6] R. Cheng, D. Littlejohn, P. Strakey, T. Sidwell, *Proc. Combust. Inst.* 32 (2) (2009) 3001–3009.
[7] M. Fairweather, M.P. Ormsby, C.G.W. Sheppard, R. Woolley, *Combust. Flame* 156 (4) (2009) 780–790.
[8] S. Daniele, P. Jansohn, J. Mantzaras, K. Boulouchos, *Proc. Combust. Inst.* 33 (2) (2011) 2937–2944.
[9] T. Kitagawa, T. Nakahara, K. Maruyama, K. Kado, A. Hayakawa, S. Kobayashi, *Int. J. Hydrogen Energy* 33 (20) (2008) 5842–5849.
[10] C.K. Law, *Combustion Physics*, Cambridge University Press, New York, 2006.
[11] V. R. Kuznetsov; V. A. Sabel'nikov, in: Turbulence and Combustion, V. R. Kuznetsov; V. A. Sabel'nikov; P. A. Libby, (Eds.) Hemisphere Publishing Corporation: Moscow, 1986; p 362.
[12] V. P. Karpov; A. N. Lipatnikov; V. L. Zimont, in: Advances in Combustion Science. In honor of Ya. B. Zel'dovich, W. A. Sirignano; A. G. Merzhanov; L. De Luca, (Eds.) AIAA: Reston, VA, 1997; Vol. 173, pp 235–250.
[13] F. Dinkelacker, B. Manickam, S.P.R. Muppala, *Combust. Flame* 158 (9) (2011) 1742–1749.
[14] P. Venkateswaran, A. Marshall, D.H. Shin, D. Noble, J. Seitzman, T. Lieuwen, *Combust. Flame* 158 (8) (2011) 1602–1614.
[15] G. Damköhler, *Zeitschrift Electrochem.* 46 (1940) 601–626.
[16] A.N. Lipatnikov, J. Chomiak, *Combust. Sci. Technol.* 137 (1–6) (1998) 277–298.
[17] H.G. Im, J.H. Chen, *Proc. Combust. Inst.* 28 (2) (2000) 1833–1840.
[18] H. Kobayashi, T. Tamura, K. Maruta, T. Niioka, F.A. Williams, *Proc. Combust. Inst.* 26 (1) (1996) 389–396.
[19] F. Gouldin; R. K. Cheng International Workshop on Premixed Turbulent Flames. http://eetd.lbl.gov/aet/combustion/workshop/workshop.html.
[20] A. Marshall, P. Venkateswaran, D. Noble, J. Seitzman, T. Lieuwen, *Exp. Fluids* 51 (3) (2011) 611–620.
[21] A. Marshall; P. Venkateswaran; J. Seitzman; T. Lieuwen, ASME Conference Proceedings 2012 (To Appear) (2012).
[22] R. J. Kee; J. F. Grcar; M. Smooke; J. Miller, Sandia National Laboratories Report SAND85-8240, Sandia National Laboratories, Livermore (1983).

[23] S.G. Davis, A.V. Joshi, H. Wang, F. Egolfopoulos, *Proc. Combust. Inst.* 30 (1) (2005) 1283–1292.
[24] N. Peters, *J. Fluid Mech.* 384 (1999) 107–132.
[25] R.J. Kee, J.A. Miller, G.H. Evans, G. Dixon-Lewis, *Proc. Combust. Inst.* 22 (1) (1989) 1479–1494.
[26] C.K. Wu, C.K. Law, *Proc. Combust. Inst.* 20 (1) (1985) 1941–1949.
[27] W. Peiyong; S. Hu; J. A. Wehrmeyer; R. W. Pitz, in: 42nd AIAA Aerospace Sciences Meeting and Exhibit, AIAA: AIAA-2004-148, Rena, NV, 2004.
[28] F.N. Egolfopoulos, *Proc. Combust. Inst.* 25 (1) (1994) 1375–1381.
[29] T. Poinsot, D. Veynante, *Theoretical and Numerical Combustion*, RT Edwards, Inc., Philadelphia, 2005.